Tel:+86-13501775977
Mail: HZ021@QQ.COM

Rev 1.4

Application Note:

TDPS250E2D2 All-in-One Power Supply Evaluation Board

1. Introduction

Transphorm has designed a complete 250 W power supply evaluation board specifically to meet the requirements for an all-in-one computer. The Power Supply combines a PFC input stage with an LLC DC-DC converter, using ON Semiconductor control ICs (NCP4810, NCP1654, NCP1397, NCP432) together with three Transphorm 600 V GaN high electron mobility transistors (HEMTs).

The compact-size board showcases GaN devices' advantage in delivering both small size and high efficiency not possible with existing silicon solutions. It is designed to switch at 200 kHz in order to shrink the size and maintain high efficiency. With universal AC input, the All-in-One Power Supply Evaluation Board can deliver up to 20 A from the 12 V output with a peak efficiency of 95.4% from a 230 V ac line. The evaluation board is shown in Fig. 1.

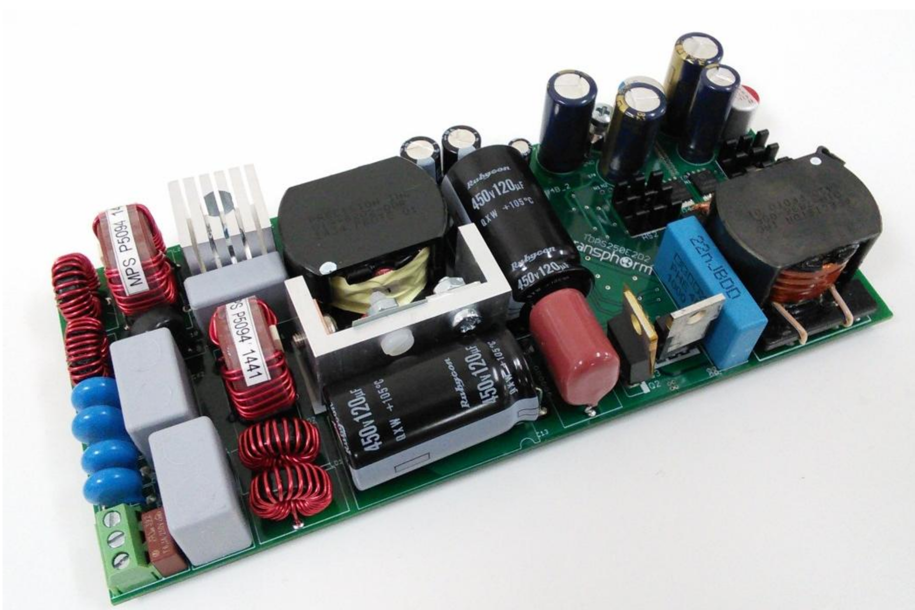

Fig. 1. All-in-One Power Supply Evaluation Board

2. TDPS250E2D2 Input/output Specifications:

- Universal AC Input: 90-265Vac;
- Output: 12Vdc at 20A;
- PFC PWM Frequency: 200kHz;
- LLC Switching Frequency: 170kHz to 250 kHz ;

3. Circuit Description for the All-in-One Power Supply

Figure 2 illustrates the topology of the power supply. Three basic functions are shown: an input EMI filter, a boost-mode PFC circuit, and an LLC DC-DC converter. Not shown is a 12V DC regulator which provides power to the PFC and LLC controllers. The link between the PFC and LLC is a 390V DC voltage, identifiable in the schematic as the voltage across capacitor C1.

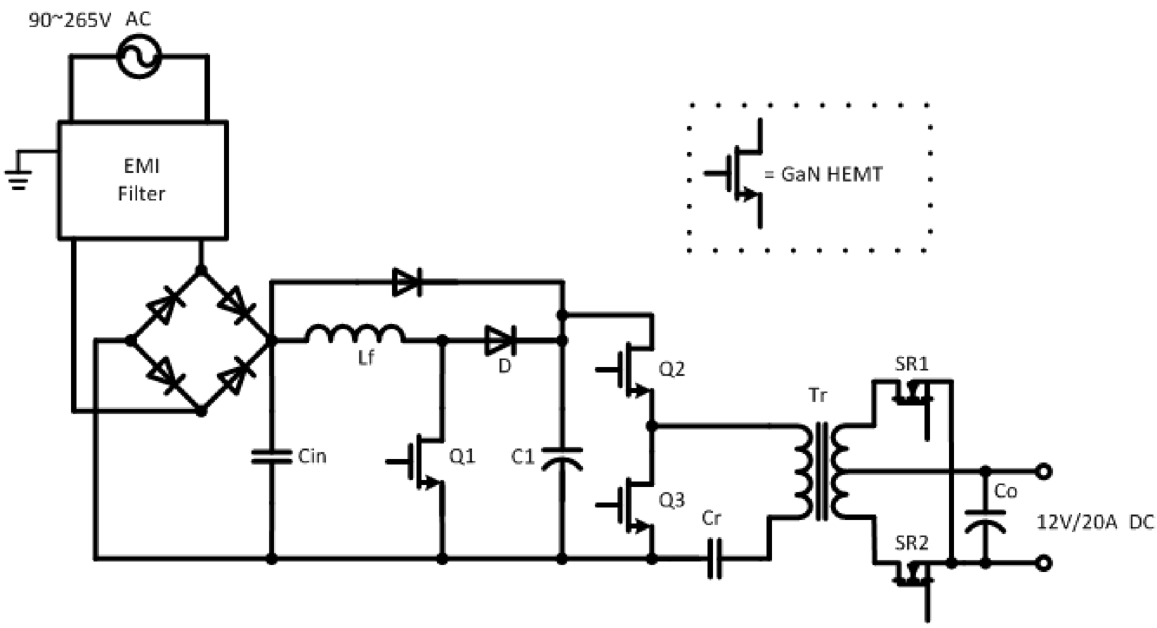

Figure 2: Simplified schematic for the complete power supply

The detailed schematic is included in pdf form with the kit documentation. The bill of materials is provided in Table I.

While a typical Si MOSFET has a maximum dV/dt rating of 50V/ns, the Transphorm GaN HEMT will switch at dV/dt of 100V/ns or higher. At this level of operation, even the layout becomes a significant contributor to performance. Figure 3 shows the layout of the layers in the evaluation board. The recommended layout minimizes the gate drive loop for each HEMT; it also keeps the traces between the switching nodes very short, with the shortest practical return trace to power ground. As the power ground plane provides a large cross sectional area to achieve an even ground potential throughout the circuit. Note that Transphorm GaN HEMTs in TO220 packages have a pin configuration of G-S-D, as opposed to the traditional MOSFET configuration of G-D-S. Placement of the source pin in the center reduces coupling between the input and output loops.

(a) Top layer

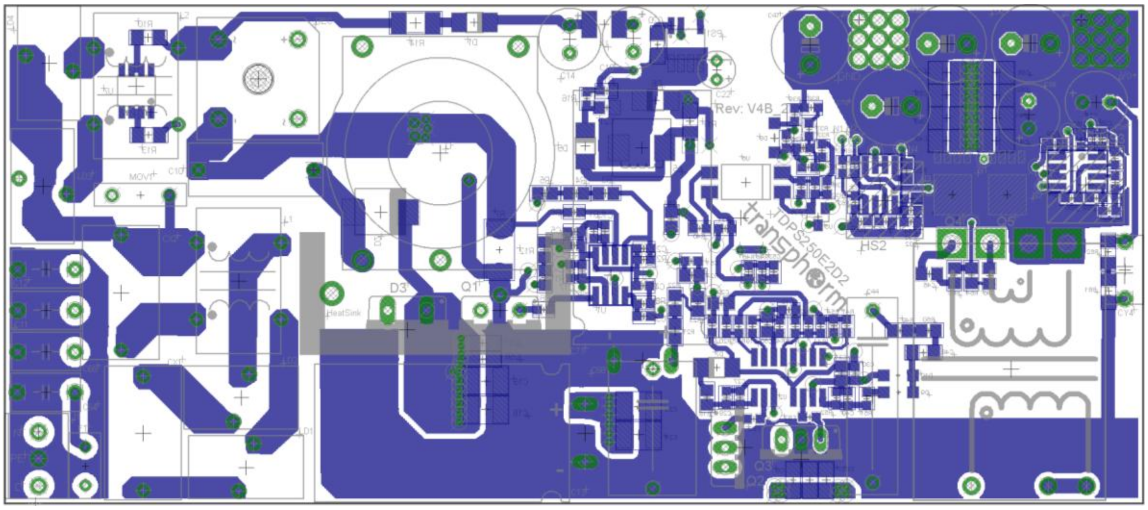

(b) Bottom layer

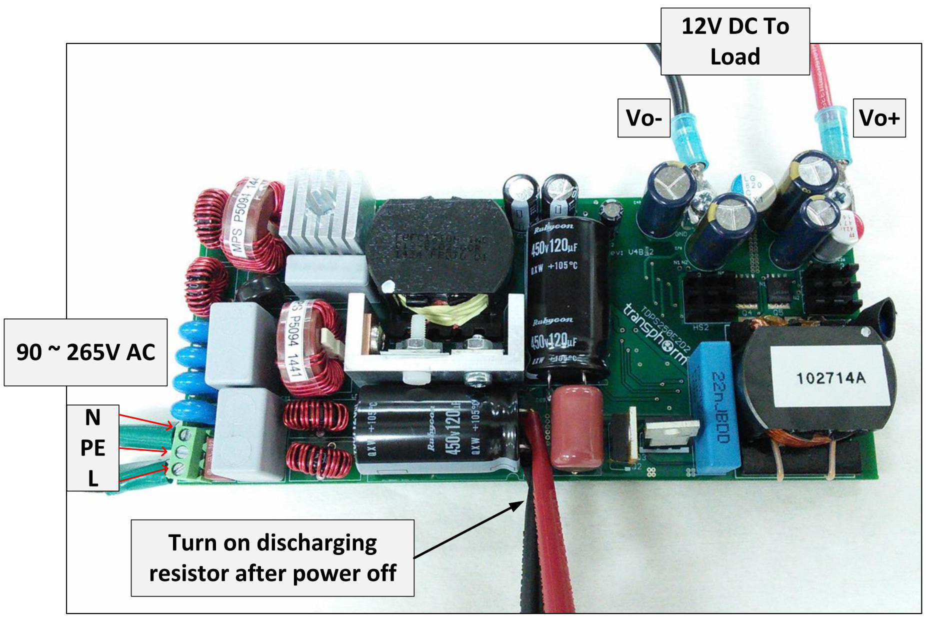

(c) Connections

Figure 3. PCB layers. Size: 5.84 inch × 2.55 inch (148mm x 64.8mm)

Table I. Bill of Materials for the All-in-One Power Supply Evaluation Board

Items	Qty	Reference	Part Description	Manufacture	Part No.
1	2	C1, C53	CAP., X7R, 2.2nF, 16V, 10%, 0603	AVX	0603YC222KAT2A
2	6	C2, C9, C28, C32, C34, C52	CAP., X7R, 1µF, 16V, 10%, 0603	Taiyo Yuden	EMK107B7105KA-T
3	1	C3	CAP., X7R, 1.5nF, 16V, 10%, 0603	Kemet	C0603C152K4RACTU
4	1	C4	CAP., X5R, 2.2µF, 16V, 10%, 0603	TDK	C1608X5R1C225K080AB
5	1	C5	CAP., NP0, 100pF, 50V, 5%, 0603	AVX	C1608C0G1H101J080AA
6	3	C6, C7, C8	CAP., NP0, 4.7nF, 630V, 5%, 1206	TDK	C3216C0G2J472J085AA
7	1	C10	CAP., Film, 0.22µF, 630V, 20%,7x15x17.5(mm)	Vishay	BFC233820224
8	5	C11, C12, C64, C65, CY4	CAP., X1Y2, 4.7nF, 250VAC, 20%, Rad.	Kemet	C947U472MYVDBA7317
9	2	C13, C71	CAP., Alum., 120µF, 450V, 20%, Rad. 18x33.5(mm)	Rubycon	450QXW120MEFC18X31.5
10	2	C14, C18	CAP., Alum., 3.3µF, 400V, 20%, E3.5-8	Rubycon	400LLE3R3MEFC8X11R5
11	5	C17, C19, C27, C37, C35	CAP., X7R, 0.1µF, 16V, 10%, 0603	Murata	GRM188R71C104KA01D
12	4	C15, C16, C23, C24	CAP., X7R, 0.1µF, 630V, 10%, 1812	TDK	C4532X7R2J104K230KA
13	1	C20	CAP., X7R, 0.1µF, 25V, 10%, 1206	Kemet	C1206F104K3RACTU
14	2	C21, C29	CAP., X5R, 10µF, 16V, 20%, 0805	Kemet	C0805C106M4PACTU
15	1	C22	CAP., Alum., 100µF, 16V, 20%, Rad. 5x2(mm)	Rubycon	16PX100MEFCTA5X11
16	1	C26	CAP., Poly. Alum., 470µF, 16V, 20%, E3.5-8	Nichicon	RNE1C471MDN1PX
17	3	C31, C50, C59	CAP., X5R, 4.7µF, 16V, 10%, 0805	Kemet	C0805C475K4PACTU
18	1	C36	CAP., X7R, 68nF, 16V, 10%, 0603	Yageo	CC0603KRX7R7BB683
19	3	C38, C47, C70	CAP., Alum., 820µF, 16V, 20%, E5-10.5	Panasonic	EEU-FC1C821
20	1	C39	CAP., Alum., 680µF, 16V, 20%, E3.5-8	Panasonic	EEU-FC1C681L
21	8	C40, C41, C42, C43, C55, C56, C62, C63	CAP., X5R, 100µF, 16V, 20%, 1210	Taiyo Yuden	EMK325ABJ107MM-T
22	1	C44	CAP., Film, 22nF, 1kV, 5%, 26x6.5(mm)	Kemet	PHE450PD5220JR06L2
23	2	C45, C46	CAP., NP0, 330pF, 50V, 5%, 0805	Kemet	C0805C331J5GACTU
24	1	C51	CAP., X7R, 10nF, 16V, 10%, 0603	TDK	CGJ3E2X7R1C103K080AA
25	1	C54	CAP., X7R, 1nF, 16V, 5%, 0603	Kemet	C0603C102J4RACTU
27	2	C57, C58	CAP., NP0, 8.2nF, 630V, 5%, 1206	TDK	C3216C0G2J822J160AA
29	1	C60	CAP., Poly. Alum., 820µF, 16V, 20%, E5-10.5	Nichicon	PLG1C821MDO1
30	1	C68	CAP., Film, 2.2µF, 450V, 5%, 18.8x12.8(mm)	Panasonic	ECW-F2W225JA
31	2	CX1, CX2	CAP., Film, 470nF, 630V, X2	Vishay	BFC233920474
32	1	R1	RES., 110k, 0.1W, 1%, 0603	Vishay	CRCW0603110KFKEA
33	1	R2	RES., 75k, 0.1W, 5%, 0603	Vishay	CRCW060375K0JNEA
34	3	R3, R4, R5	RES., 2.37M, 1/8W, 1%, 0805	Yageo	RC0805FR-072M37L
35	1	R6	RES., 3.3k, 0.1W, 1%, 0603	Stackpole	RMCF0603FT3K30
36	1	R7	RES., 60mΩ, 1W, 1%, 2512	Vishay	WSL2512R0600FEA
37	2	R8, R34	RES., 11k, 0.1W, 1%, 0603	Panasonic	ERJ-3EKF1102V

38	2	R9, R38	RES., 23.2k, 0.1W, 1%, 0603	Panasonic	ERA-3AEB2322V
39	2	R10, R13	RES., 220k, 1/4W, 1%, 1206	Yageo	RC1206FR-07220KL
40	1	R12	RES., 1.8M, 1/8W, 1%, 0805	Rohm	KTR10EZPF1804
41	1	R11	RES., 1.78M, 1/8W, 1%, 0805	Vishay	CRCW08051M78FKEA
42	1	R14	RES., 10Ω, 2W, 2%, 2512	Vishay	RCL122510R0FKEG
43	1	R15	RES., 2.05k, 0.1W, 1%, 0603	Yageo	RC0603FR-072K05L
44	1	R16	RES., 13k, 0.1W, 1%, 0603	Yageo	RC0603FR-0713KL
45	1	R17	RES., 13k, 1/4W, 5%, 1206	Panasonic	ERJ-8GEYJ133V
46	1	R18	RES., 4.7Ω, 1/8W, 1%, 0805	Rohm	KTR10EZPF4R70
47	1	R19	RES., 4.32k, 0.1W, 1%, 0603	Panasonic	ERJ-3EKF4321V
48	1	R20	RES., 4.7k, 0.1W, 1%, 0603	Yageo	RC0603FR-074K7L
49	3	R21, R22, R23	RES., 953k, 1/8W, 1%, 0603	Panasonic	ERJ-6ENF9533V
50	1	R24	RES., 10k, 1/8W, 1%, 0805	Panasonic	ERJ-6ENF1002V
51	2	R25, R27	RES., 20k, 0.1W, 1%, 0603	Rohm	MCR03ERTF2002
52	2	R26, R30	RES., 5.9k, 0.1W, 1%, 0603	Yageo	RC0603FR-075K9L
53	2	R28, R29	RES., 0.56Ω, 1/8W, 1%, 0805	Yageo	RL0805FR-070R56L
54	1	R31	RES., 2.2k, 0.1w, 1%, 0603	Yageo	RC0603FR-072K2L
55	2	R32, R40	RES., 1k, 0.1W, 1%, 0603	Yageo	RC0603FR-071KL
56	1	R33	RES., 14.7k, 0.1W, 1%, 0603	Panasonic	ERJ-3EKF1472V
57	1	R35	RES., 13.7k, 0.1W, 1%, 0603	Panasonic	ERJ-3EKF1372V
58	1	R36	RES., 750Ω, 0.1W, 1%, 0603	Yageo	RC0603FR-07750RL
59	1	R37	RES., 249Ω, 0.1W, 1%, 0603	Vishay	MCR03ERTF2490
60	1	R39	RES., 100Ω, 0.1W, 1%, 0603	Yageo	RC0603FR-07100RL
61	1	R41	RES., 7.5k, 0.1W, 1%, 0603	Yageo	MCR03ERTF7501
62	2	R42, R46	RES., 2k, 0.1W, 1%, 0603	Panasonic	ERJ-3EKF2001V
63	1	R43	RES., 150k, 0.1W, 1%, 0603	Yageo	RC0603FR-07150KL
64	1	R44	RES, 12.4k, 0.1W, 1%, 0603	Yageo	RC0603FR-0712K4L
65	6	R47, R48, R57, R58, R59, R60, R51	RES.,N/A, 0603	N/A	
66	1	R45	RES, 6.8k, 0.1W, 1%, 0603	Yageo	RC0603FR-076K8L
67	3	R53, R56, R52	RES., 0Ω, 0.1W, 0603	Yageo	RC0603JR-070RL
68	2	R49, R50	RES., 24k, 1/8W, 5%, 0805	Yageo	RC0805JR-0724KL
69	2	R54, R55	RES., 4.7Ω, 0.1W, 1%, 0603	Panasonic	P4.7AJCT-ND
70	2	R61, R62	RES., 2.2M, 1/4W, 5%, 1206	Yageo	RC1206JR-072M2L
71	2	R63, R64	RES., 10Ω, 1/4W, 5%, 0805	Stackpole	RPC0805JT10R0
72	1	D1	Diode, 1000V, 1A, DO-214AC	Diode Inc	S1M-13-F
73	1	D2	Diode, 600V, 3A, DO-214AB	Fairchild	S3J
74	1	D3	Diode, SiC, 600V, 2A, TO220-2	Cree	C3D02060A
75	1	D5	Diode, 600V, 1A, DO-214AC	Diode Inc	S1J-13-F
76	1	D6, D7	Diode, Ultra Fast, 600V, 1A, DO-214AC	Diode Inc	ES1J-LTP
77	1	D8	Diode, Zener, 11V, 0.5W, SOD123	On-Semi.	MMSZ5241BT1G
78	2	D9, D10	Diode, 75V, 0.15A, SOD323F	Fairchild	1N4148WS
79	3	Q1, Q2, Q3	GaN HEMT, 600V, 9A, TO220	Transphorm	TPH3002PS
80	4	Ld1, Ld2, Ld3, Ld4	IND., 26µH, DCR < 40mΩ	MPS Inc.	P1131
81	2	L1, L2	Common Mode Chk, 9mH, 1.9A, 22x15(mm)	MPS Inc.	P5094
82	1	L4	IND., 1mH, 70mA, 1210	Wurth Elek.	744045102
83	1	L5	IND., 1mH, 0.235A, 7.6x7.6(mm)	Cooper Buss.	DRA73-102-R
84	1	LF	IND., 480µH, 200kHz, CC30/19	Precision	019-8202-00R
85	1	J1	CONN., 300V, 10A, 3Pin_3.5mm	Wurth Elek.	691214110003

86	2	J2, J3	BUSH, 54A	Wurth Elek.	7461093
87	2	HS2, HS3	HEATSINK, 10x10(mm)	Assmann WSW Comp.	V2017B
88	1	PS1	PowerChip, Offline, 12V, 1.44W, SO-8C	Power Integ.	LNK304DG-TL
89	1	MOV1	MOV, 504V, 3.5kA, Disc 10.5mm	Panasonic	ERZ-E08A561
90	1	U2	LLC Controller, 16-SOIC	On-Semi	NCP1397BDR2G
91	1	U1	PFC Controller, CCM, 200kHz, SO-08	On-Semi	NCP1654BD200R2G
92	2	U3,U4	Synchronous Rectifier Driver, SO-08	On-Semi	NCP4304BDR2G
93	1	U5	Voltage Reference, SOT23	On-Semi	NCP432BCSNT1G
94	1	U6	Optoisolator, 5kV, 4-SMD	Avago	HCPL-817-50AE
95	1	U7	X2 CAP. DIS., SOIC-8	On-Semi	NCP4810DR2G
96	1	F1	FUSE, SLOW, 250V, 6.3A	Littlefuse Inc	39216300000
97	2	Q4, Q5	MOSFET, N-CH, 40V, 100A, PG-TDSON-8	Infineon	BSC017N04NS G
98	1	Transformer	Transformer, LLC, 240W, 170kHz – 200kHz	Precision	019-7896-00R
99	3	FB1, FB2, FB3	Ferrite Bead, 60Ω@100MHz, 500mA, 0603	TDK	MMZ1608Y600B
100	1	REC	Rectifier Bridge, 600V, 8A, D-72	Vishay	VS-KBPC806PBF
101	1	N/A	Thermal Pad, 0.9W/m-K, 18.42x13.21(mm)	Aavid Thermalloy	53-77-9G
102	1	N/A	Ferrite Core, 47Ω@100MHz, 4.2mm OD	Wurth Elek.	74270012

*: Shaded items are not installed.

4 Circuit Descriptions for the PFC AC-DC Converter

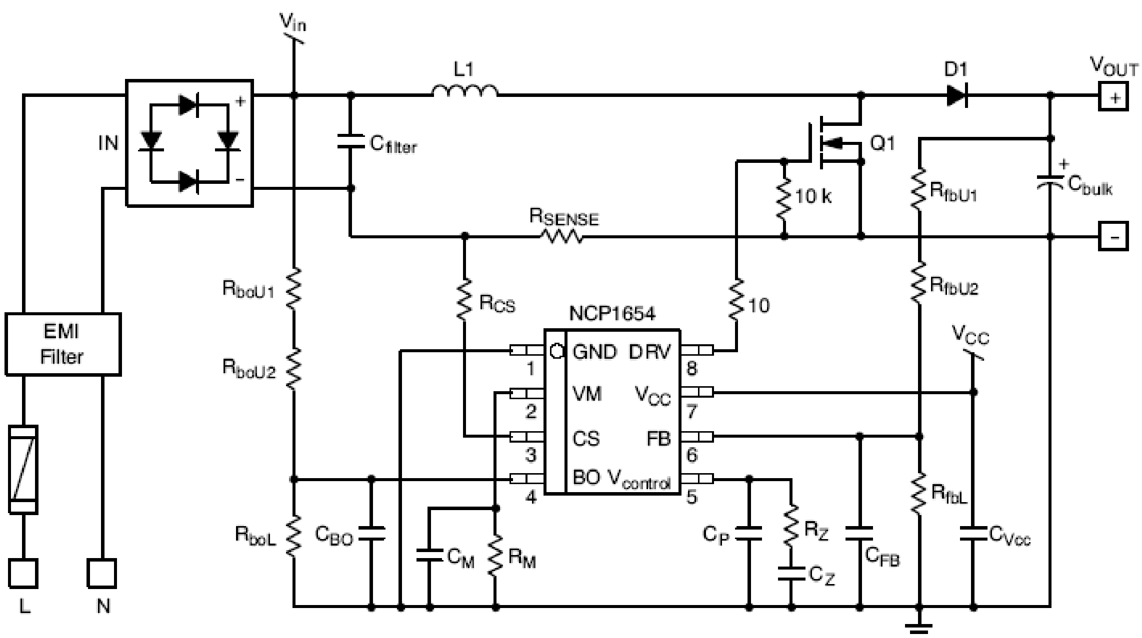

Figure 4 Generic NCP1654 Application Schematic

Please refer to the datasheet of NCP1654 and application note AND8324-D from On Semiconductor Inc. in [1, 2]. Figure 4 shows a generic NCP1654 application schematic. The parameters of PFC controller and inductor are showed in Table II and III respectively.

Table II Parameters of PFC controller

Parameters	Unit	Val	Description
f_{ac}	(Hz)	**60**	Ac line frequency
V_{acLL}	(V)	**90**	Ac line rms lowest level (generally 85 V or 90 V in wide mains applications)
V_{acHL}	(V)	**265**	Ac line rms highest level (generally 265 V in wide or European mains applications)
$V_{ac,on}$	(V)	**75**	Ac line rms voltage to start up (generally 75 Vac in wide mains applicaions)
V_{out}	(V)	**385**	Wished regulation level for the output voltage (generally 390 V or 400 V in wide mains apps)
V_{outLL}	(V)	**385**	Minimum Output Voltage you can accept in normal operation - Use VoutLL=Vout as a default value if you don't know
eff	(%)	**95**	Expected efficiency at low line, full load
P_{out}	(W)	**216**	Maximum output power
ΔI_{pk-pk}	(%)	**30**	Targeted peak to peak ripple of the coil current at low line and full load
R_{dsON}	(Ω)	**0.29**	MOSFET on-time resistance @ 25 °C
$T_{hold-up}$	(ms)	**20**	Hold-up time. Put 0 if no hold-up time is specified or if you don't know.
$(V_{out})_{min}$	(V)	**310**	Minimum output Voltage you can accept at the end of the hold-up time
$\%DV_{pk-pk}$	(%)	**3**	Peak to peak low frequency ripple that is acceptable across the bulk capacitor as a percentage of the regulation output voltage ("Vout").
Bulk Capacitor and Coil specification			
C_{bulk} cal.	(µF)	166	Minimum Cbulk capacitance meeting the low frequency ripple and hold-up time constraints (*)
C_{bulk} Selected	(µF)	**240**	Choose higher standard value
ESR of C_{bulk}	(mΩ)	150	The ESR of Cbulk
L_{calc}	(µH)	397	Proposed coil inductance
L Selected	(µH)	**480**	Your inductance choice
(I_{coil})max	(A)	4.02	Max peak coil current resulting from your inductance choice
(I_{coil})rms	(A)	2.53	Maximum rms coil current
Conduction Losses			
Input Bridge	(W)	4.5	Assuming the forward voltage of each diode is 1 V
MOSFET	(W)	2.9	Assuming that RdsON doubles at the highest junction temperature of your application

Diode	(W)	0.6	Assuming that RdsON doubles at the highest junction temperature of your application Assuming that the diode forward voltage is 1 V.
Feed-back Arrangement			
R_{fbL}	(kΩ)	**23.2**	Choose a standard value
R_{fbU1}+R_{fbU2}	(kΩ)	**3,550**	(RfbU1+RfbU2) calculated based on RfbL and Vout.
C_{fb}	(pF)	**100**	
Input Voltage Sensing	Choose high accuracy resistors for RboU1, RboU2 and RboL		
R_{boL}	(kΩ)	**24.7**	Choose a standard value < 140 kΩ
R_{boU1} + R_{boU2}	(kΩ)	**2,007**	(RboU1+RboU2) calculated based on RboL and Vac,on.
C_{bo} cal.	(µF)	1.69	Cbo calculated based on RboL and line frequency
C_{bo} Selected	(µF)	**2.20**	Choose the closest standard value.
$V_{ac,off}$ cal.	(V)	64.5	The calculated PFC brown out off thresold of AC input
Current Sense Network			
R_{sense} cal.	(Ω)	0.17	Value that makes the Rsense dissipation = (0.5% * Pout)
R_{sense} selected	(Ω)	**0.06**	Your "Rsense" choice
P_{Rsense}	(Ω)	0.4	Losses resulting from your Rsense choice
R_{cs} cal.	(kΩ)	1.3	Value resulting from your Rsense choice
R_{cs} selected	(kΩ)	**3.3**	Choose higher standard value.
R_m	(kΩ)	**110**	Value resulting from your Rsense choice
C_m	(nF)	2.2	Value resulting from your Rm choice
Compensation Arrangement			
F_c	Hz	20	The wished cross over frequency at high line.
C_z cal.	(µF)	2.0	The calculated Cz based on (G0)dB and fc.
C_z	(µF)	**2.2**	Choose closest standard value
R_z cal.	(kΩ)	25	The calculated Rz based on fz1.
R_z	(kΩ)	**11**	Choose closest standard value
C_p cal.	(nF)	**1.5**	The calculated Cp based on fp1

Table III Parameters of PFC inductor

Items	Value	Comments
Inductance	480µH	~25% ΔI_{pk_pk}
Core Type	CC30/19	Height < 20mm
Core Material	A-Core JPP-95	Similar to 3C95
Wire	40/38 Litz Wire	~0.11 Ω DCR
Winding Turns	38	<10pF winding capacitance
Air Gap	~0.42 mm	Not considered fringing effect

5 Circuit Descriptions for the LLC DC-DC Converter

Figure 4 illustrates the topology of the LLC DC-DC converter portion of the evaluation board, which is based on the NCP1397 and NCP4304 controllers. The series capacitor forms the series-parallel resonant tank with leakage and magnetic inductances in the primary side of the transformer. From this configuration, the resonant tank and the load on the secondary side, act as a voltage divider. By changing the frequency of input voltage, the impedance of resonant tank will change; this impedance will divide the input voltage with load. The primary-side switches, Q1 and Q2, are the GaN HEMTs. Transistors SD1 and SD2 on the secondary side are synchronous rectifiers to improve the performance and efficiency. As may be seen in Fig. 4, there is no need for special gate drivers for the GaN HEMTs. Further information and discussion on the fundamental circuit schematics and the characteristics of LLC DC-DC converters are provided in [3]-[5].

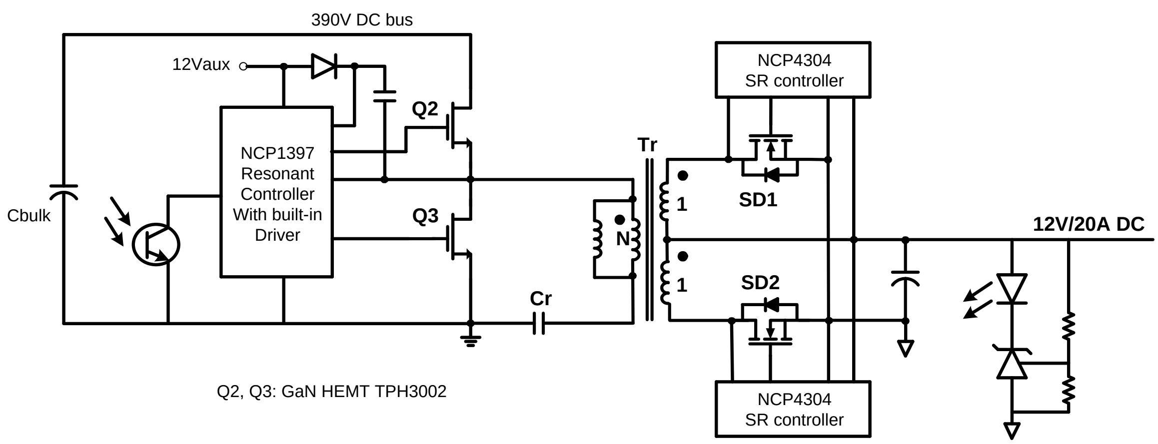

Fig .4. Circuit topology for LLC DC-DC converter using silicon MOSFETs for line rectification

Although the LLC is a resonant topology, characterized by soft switching, hard switching does nevertheless occur during start up. During this phase, the large reverse recovery charge (Qrr) of typical silicon MOSFETs causes problematic overshoot, ringing, and loss. Transphorm's

TPH3002PS 1st-generation GaN power devices show a low on-resistance of 0.29 ohm typical and are capable of reverse conduction during dead time with a low Qrr of 29nC, more than 20 times lower than state-of-the-art Si counterpart as seen in Figure 5. These features can remarkably improve the performance and efficiency of hard-switch circuits, and are also important for hard starting in resonant circuits such as the LLC topology.

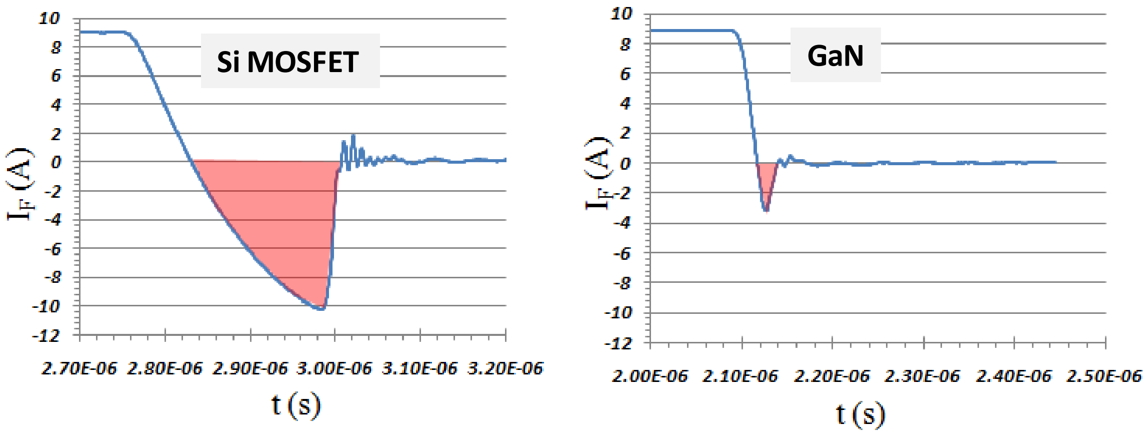

Fig.5 Reverse recovery charge test result for a Si MOSFET and a GaN HEMT with similar on resistance, showing a 20x reduction of Qrr for GaN.

Table IV gives a comparison of CoolMOS and GaN HEMT. The low Qrr will help reducing excessive spikes during start-up process in a LLC dc-dc converter.

Table IV: Comparison of GaN HEMT with equivalent CoolMOS IPP60R380C6

Parameter	TPH3002PS	IPP60R380C6
ID	9A (continuous)	10.6A (for D=0.75)
Ron	290mΩ	340mΩ
Qg	6.2nC	32nC
Eoss(400V)	3.1µJ	2.8µJ
Qrr	29nC	3.3µC

Startup sequence:

1) Connect a load; The load should be resistive, and maximum of 240watt at 12Vdc;
2) Connect an AC power source, set to the desired voltage higher than 90V.
3) Place a cooling fan facing the GaN HEMTs heat sinks of PFC and LLC (provide a minimum of 30 CFM air flow);
4) Turn on the cooling fan if output power is higher than 150W;

Probing: In order to minimize additional inductance during measurement, the tip and the ground of the probe should be directly attached to the sensing points to minimize the sensing loop; while the typical long ground lead should be avoided since it will form a sensing loop and could pick up the noise. An example of low inductance probing is shown in Fig 6. The differential probes are not recommended for the GaN signal measurement.

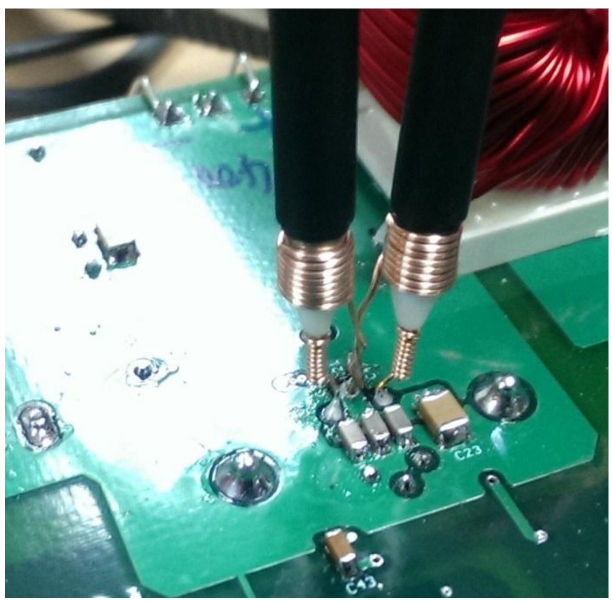

Fig. 6. Low-inductance probing of fast, high-voltage signals

Performance: Efficiency and Power Factor have been measured at low line (115Vac) and high line (230Vac) input for a range of loads on the 12Vdc output using the WT1800 precision power analyzer by Yokogawa. The results are shown in figure 7-9 for the complete power supply and for the individual LLC circuits. The mid-load efficiency is more than 94% at low line and about 95.4% at high line, which is noticeably better than commercial boards with Si switches.

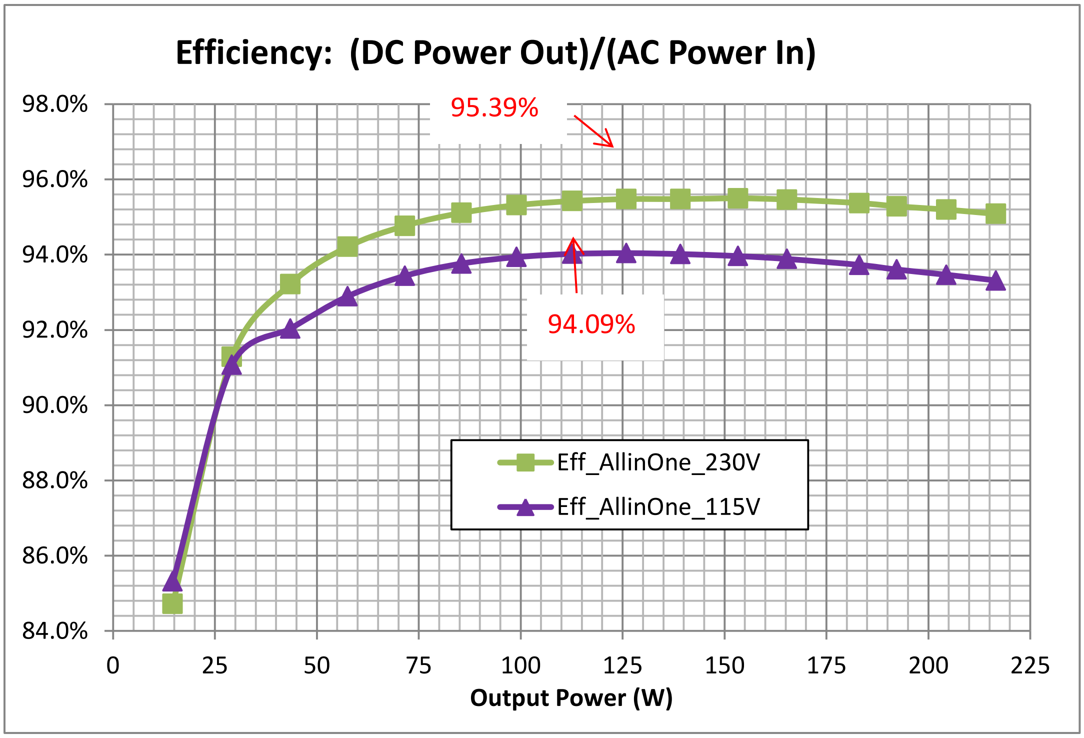

Figure 7. Efficiency for the power supply at 115V and 230V input

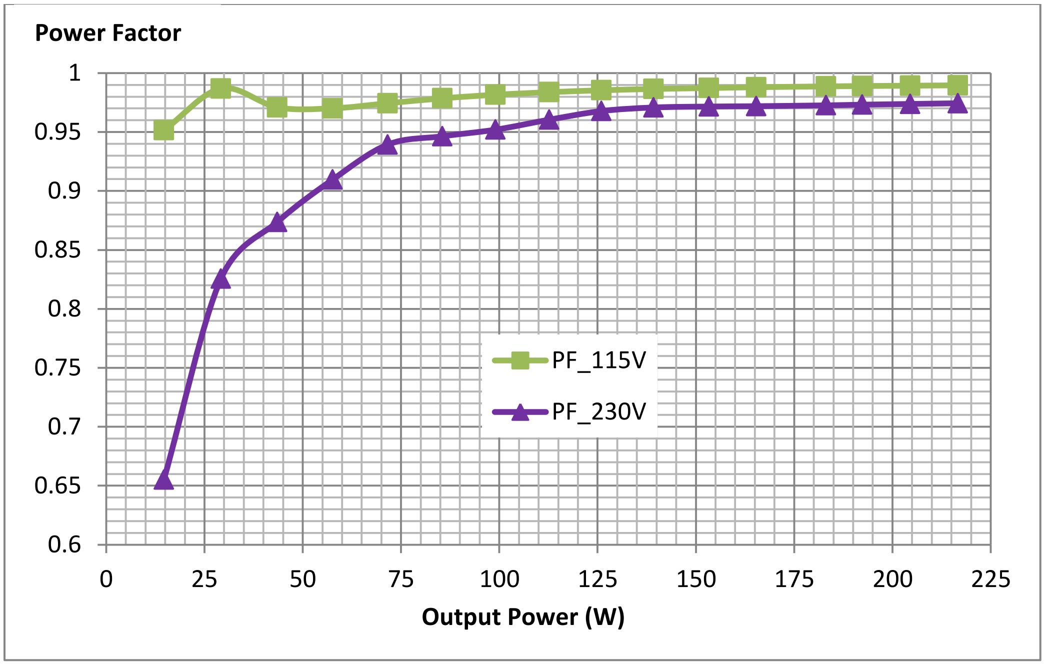

Figure 8. Power Factor vs. Output Power at 115V and 230V input

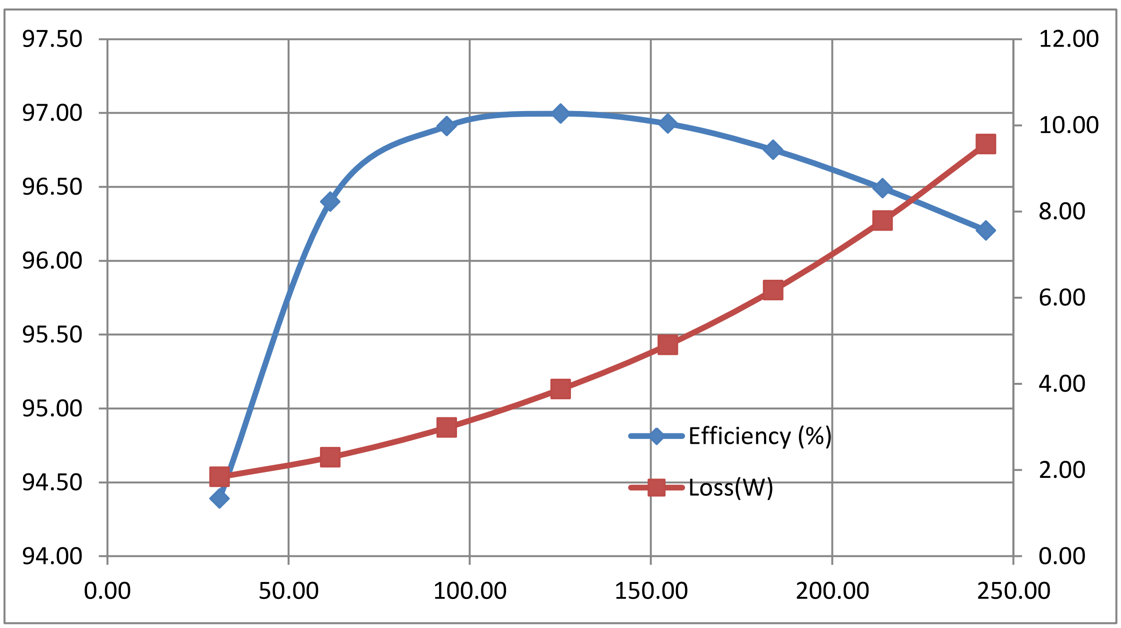

Figure 9. The efficiency result for the LLC DC/DC Converter circuit at 390Vdc input to 12Vdc output

Conducted emissions have also been measured for this board using a LIN-115A LISN by Com-Power. The results compared to EN55022B limits are shown in figure 10.

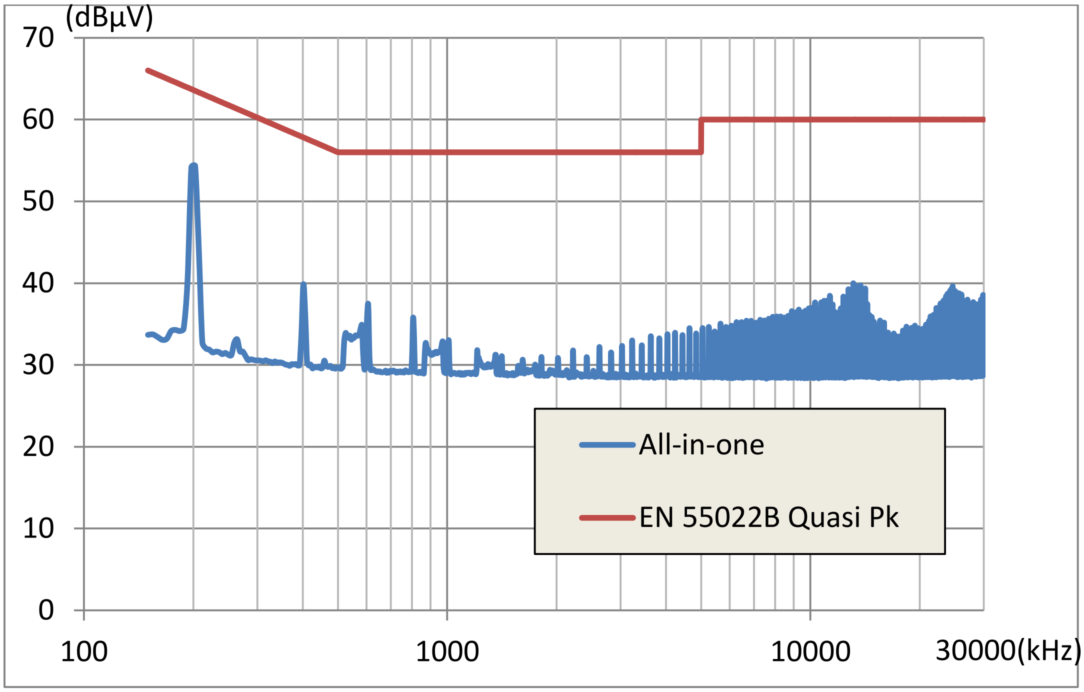

Figure 10. Conducted emissions @115V AC, 240W Load

Standby power consumption is not optimized in this design for showing the superior performance over Si-based devices. Current Controlled Frequency Foldback (CCFF) and burst mode methods can be applied for very low power loss requirement at zero and light load using corresponding controllers and circuits.

WARNING: There are no specific current or voltage protection on this board; users need to follow the test procedure and operation limits carefully.

REFERENCES:

[1]. Datasheet of NCP1654, website: www.onsemi.com, On Semiconductor.

[2]. AND8324-D Application Note, website: www.onsemi.com, On Semiconductor.

[3]. Robert L. Steigerwald, "A Comparison of Half-bridge resonant converter topologies," *IEEE Transactions on Power Electronics*, Vol. 3, No. 2, pp. 174-182, April 1988.

[4]. Bo Yang, F.C. Lee, A.J. Zhang, H. Guisong, "LLC resonant converter for front end DC/DC conversion" *Proc. IEEE APEC'02*, pp.1108 – 1112, 2002.

[5]. B. Lu, W. D. Liu, Y. Liang, F. C. Lee, and J. D. VanWyk, "Optimal design methodology for LLC resonant converter," *Proc. IEEE APEC'06*, pp. 19–23, 2006.